Super Resolution Imaging via Sparse Interpolation in Wavelet Domain with Implementation in DSP and GPU

H. Chavez[1], V. Gonzalez[1], A. Hernandez[2], and V. Ponomaryov[1]

[1] Instituto Politécnico Nacional, ESIME-Culhuacan, México, D.F., México
charomi0880@yahoo.com.mx,
alx3416@hotmail.com, vponomar@ipn.mx
[2] Estudios de Posgrado de la ciudad de México, D.F., México
ariiitta@gmail.com

Abstract. This paper focuses on a novel image resolution enhancement method employing the wavelet domain techniques and hardware implementation of designed framework. In novel resolution enhancement approach for better preservation of the edge features, additional edge extraction step is used employing high-frequency (HF) sub-band images - low-high (LH), high-low (HL), and high-high (HH) - via the Discrete Wavelet Transform (DWT). In the designed procedure, the low resolution (LR) image is used in the sparse interpolation for the resolution-enhancement obtaining low-low (LL) sub-band. An efficiency analysis of the designed and other state-of-the-art filters have been performed on the DSP TMS320DM648 by Texas Instruments through MATLAB's Simulink module and on the video card (NVIDIA Quadro K2000), demonstrating that novel SR procedure can be used in real-time processing applications. Experimental results have confirmed that implemented framework outperforms existing SR algorithms in terms of objective criteria as well as in subjective visual perception, justifying better image resolution.

Keywords: super-resolution, edge extraction, wavelet transform, sparse interpolation, DSP, GPU.

1 Introduction

Exist recent advances in low-cost imaging solutions and increasing storage capacities; there is an increased demand for better image quality in a wide variety of applications involving both image and video processing. While it is preferable to acquire image data at a higher resolution to begin with, one can imagine a wide range of scenarios where it is technically not feasible. In some cases, it is the limitation of the sensor due to low-power requirements as in satellite imaging, remote sensing, radar, CCDs and surveillance imaging [1].

In remote sensing monitoring and in navigation missions, with small airborne or unmanned flying vehicle platforms, LR sensors with simple and cheap hardware, such as unfocused SAR systems, optical cameras are using but cheap sensors sacrifice spatial resolution; additionally, the uncertainties that are connected with attributed to

E. Bayro-Corrochano and E. Hancock (Eds.): CIARP 2014, LNCS 8827, pp. 973–981, 2014.

random signal perturbations and imperfect system calibration additionally decrease the image resolution [2], [3].

The general image capture model combines the various effects of the digital image acquisition process such as point-wise blurring, motion, under-sampling, and measurement noise. The problem in this point is to estimate an HR image $x(i,j)$ from measurements of an LR image $y(i,j)$ that were obtained through a linear operator K that forms a degraded version of the unknown HR image, which was additionally contaminated by an additive noise $\mathcal{E}(i,j)$, and can be represented as the forward imaging model as follows:

$$y(i,j) = K[x(i,j)] + \mathcal{E}(i,j), \tag{1}$$

In most applications, K is a subsampling operator that should be inverted to restore an original image size and this problem usually should be treated as an ill-posed problem. Current proposal introduces a general class of nonlinear inverse estimators that were obtained with an adaptive mixing of linear estimators, with applications to image interpolation.

Image resolution enhancement using wavelets is a relatively new subject, and recently, many novel algorithms have been proposed [4, 5]. These algorithms have attempted to improve the sharpness and fine features by using special procedures in the wavelet domain where such reconstructions are performed by manipulations in the different decomposition sub-bands.

The principal contributions of current SR proposal in difference to other state-of-the-art resolution-enhancement techniques consists of the mutual interpolation via Lanczos algorithm, which has good approximation capabilities [6], and nearest neighbor interpolation (NNI) technique, which uses the closest pixels to an approximation point, and edge extraction procedure in wavelet transform space with adaptive directional LR image interpolation via sparse image mixture models in a DWT frame. The proposed framework additionally applies special denoising filtering based on the *Non-Local Means* (NLM) for the input LR image performing better robustness in the resolution enhancement process. Finally, all of the sub-band WT images are combined, generating a result HR image via IDWT demonstrating better resolution performance in terms of the objective criteria and subjective perception in comparison with the best existing algorithms.

To justify that the novel algorithm of image resolution enhancement has real advantages, we have compared the proposed SR procedure with other similar techniques, such as: *Demirel-Anbarjafari Super Resolution* (DASR) [7], *Wavelet Domain Image Resolution Enhancement Using Cycle-Spinning* (WDIRECS) [8], *Image Resolution Enhancement applying Discrete and Stationary Wavelet Decomposition* (IREDSWD) [9], and *Discrete Wavelet Transform-Based Satellite Image Resolution Enhancement* (DWTSIRE) [10]. Numerous aerial optical, SAR and medical images from [11] and [12] databases that have different nature and physical characteristics were studied applying the designed and better existing SR procedures.

The remainder of this paper is organized as follows. Section 2.1 presents a short introduction to the NLM filtering method, and Section 2.2 shows an implementation of an image interpolation through the inverse mixing estimator. The proposed technique

for SR image reconstruction is presented in Section 3. Section 4 discusses the qualitative and quantitative results of novel technique in comparison with other better conventional techniques. In section 5, the real time implementation of the proposed and promising SR techniques are explained. And finally; the conclusions are drawn in Section 6.

2 Problem Statement of Proposed Methodology

2.1 Non-Local Means Denoising

The NLM technique that we use in initial denoising stage is based on the assumption that the image content is likely to repeat itself within some neighborhood in the image. The NLM algorithm computes a denoised pixel $\hat{x}(i,j)$ by applying the weighted mean of the surrounding pixels of $y(i,j) = \{y(r,s)|(r,s) \in N(i,j)\}$, the estimated value for a pixel (i,j), is computed as a weighted average of all the pixels in the image [13]:

$$\hat{x}(i,j) = \frac{\sum_{(r,s)\in N(i,j)} y[r,s]w[i,j;r,s]}{\sum_{(r,s)\in N(i,j)} w[i,j;r,s]}, \tag{2}$$

where $N(i,j)$ stands for the neighborhood of the pixel $y[r,s]$, and the term $w[i,j;r,s]$ is the weight for the *(i,j)-th* neighbor pixel.

The weights for the filter are computed based on radiometric (gray-level) similarity and geometric similarity between the pixels, namely:

$$w[i,j;r,s] = exp\left\{-\frac{(y[i,j]-y[r,s])^2}{2\Delta^2}\right\} \cdot G\left(\sqrt{(i-r)^2+(j-s)^2}\right), \tag{3}$$

where the function *G* takes the geometric distance into account and the parameter Δ controls the effect of the grey-level difference between the two pixels. This way, when the two pixels that is markedly different, the weight is very small, implying that this neighbor is not to be trusted in the averaging. The denoised image $\hat{x}(i,j)$ is used in next steps of the proposed framework.

2.2 Interpolations with Sparse Wavelet Mixtures

The subsampled image $\hat{x}(i,j)$ is decomposed with one level DWT in the sub-bands (LL, LH, HL, HH), which are treated as the matrixes H whose columns (approximations and details) are the vectors of a wavelet frame on a single scale. A construction is performed with a dual frame matrix H whose columns are the dual wavelet frames $\{h_{i,j}\}_{0\le i\le 3}$. The wavelet coefficients are written as follows:

$$\hat{z}(i,j) = \langle \hat{x}, h_{i,j} \rangle = H\hat{x}(i,j). \tag{4}$$

The WT separates an LF image (an approximation) z_l that is projected over the sub-band image *LL* scaling filters $\{h_{0,j}\}_{j\in\mathcal{G}}$ and an HF image (details) z_h that is projected over the finest scale wavelets *LH*, *HL*, and *HH* in three directions $\{h_{i,j}\}_{1\le i\le 3, j\in\mathcal{G}}$.

The LF image z_l has little aliasing, and it can be interpolated sufficiently well when applying a *Lanczos* interpolator V^+. For interpolating the HF image z_h, we employ directional interpolators V_θ^+ for $\theta \epsilon \Theta$, where Θ is a set of angles that is uniformly discretized between 0 and π.

$$z_l = \sum_{j \epsilon \mathcal{G}} \hat{z}(0,j) h_{0,j} \quad and \quad z_h = \sum_{i=1}^{3} \hat{z}(i,j) h_{i,j}. \tag{5}$$

For each angle θ, a directional interpolator V_θ^+ is applied over a block $D = D_{\theta,q}$ that is interpolated with a directional interpolator $V_D^+ = V_\theta^+$. The HF z_h and LF z_l images are interpolated with a separable and *Lanczos* interpolator V^+. The resulting interpolator can be written in the following form [14]:

$$U_{LL} = V^+ \hat{z}(i,j) + \sum_{\theta \epsilon \Theta} (V_\theta^+ - V^+) \, \bar{\mathrm{H}} \left(\sum_{q \epsilon \hat{z}_\theta} \bar{a} \, (D_{\theta,q}) l_{D_{\theta,q}} \hat{z}(i.j) \right). \tag{6}$$

For each angle θ, an update is computed over wavelet coefficients of each block of direction θ multiplied by their mixing weight $\bar{a}(D_{\theta,q})$, with the difference between the separable interpolator V^+ and a directional interpolator V_θ^+ along θ. This overall interpolator is calculated with $O(|\Theta|N)$ operations, where number of interpolation angles $|\Theta|$ was 20 in performed numerical experiments, with blocks having a width of 2 pixels and a length between 6 and 12 pixels depending on their orientation.

3 Designed SR Technique

In designed framework, one level DWT applying different wavelet families is used to decompose an input image. DWT separates an image into different sub-band (LL, LH, HL, and HH) images where LH, HL and HH sub-bands contain the HF image component. The interpolation process should be applied to all these sub-band images. Additionally, in the denoising stage, the NLM filter from (2) is applied, the neighborhood *y* is used in the simulation as 5x5 pixels, and the parameter $\Delta = 2$ is chosen in Noise Reduction Stage (Fig.1).

In the proposed SR procedure, the LR image is used as the input data in the sparse representation for the resolution-enhancement process during Sparse Stage (Fig.1) where the algorithm computes the missing samples along the direction θ from the previously calculated new samples, following the entire sparse process is performed with the *Lanczos* interpolation, reconstructing LL sub-band.

The calculated difference between the interpolated LL sub-band image (with factor 2) and the LR input image are in their HF components that why it has been proposed the intermediate process to correct the estimated HF components applying this difference image. In designed framework (Fig.1), this difference is performed in HF sub-bands by interpolating each band via NNI process, including additional HF features into the HF images. It has been noticed that this intermediate process generates a significantly sharper reconstructed SR image. This sharpness is boosted by the fact that the interpolation of the isolated HF components in HH, HL, and LH appears to preserve more HF components than interpolating from the LR image directly.

To preserve edges and to obtain a sharper enhanced image, we have proposed an extraction step of the edges using HF sub-bands images, following the edge information is used into HF sub-bands employing NNI during *Edge Extraction Stage* (Fig.1). The edge extracted image is calculated as follows [15]:

$$S = \sqrt{(HH)^2 + (HL)^2 + (LH)^2}, \tag{7}$$

Finally, we perform an additional interpolation with *Lanczos* interpolation (factor 2) to obtain the requized size for the IDWT during *IDWT* and *SR Stage* (Fig.1).

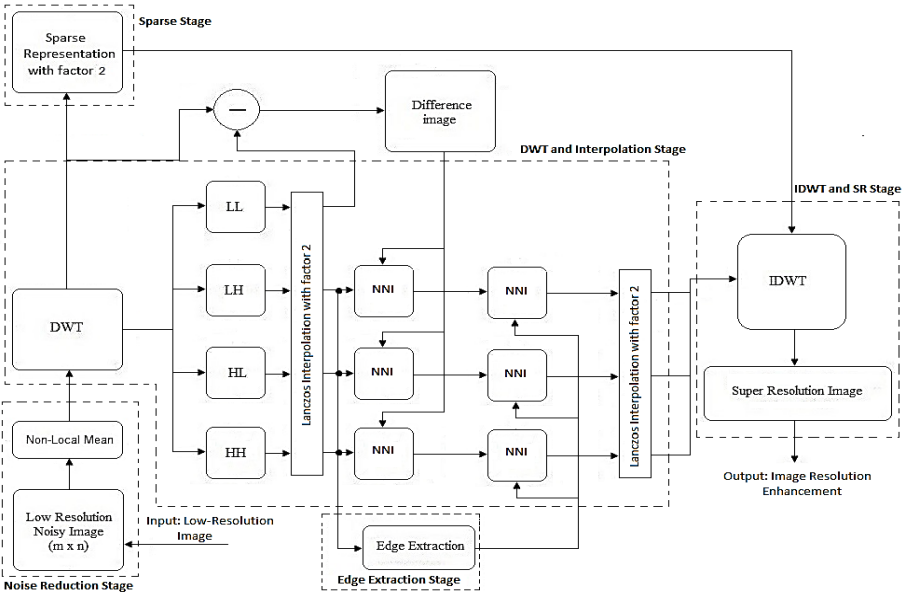

Fig. 1. Block diagram of the proposed super-resolution algorithm

4 Experimental Results and Discussion

In order to show the effectiveness of the proposed method over the conventional and state-of-the-art image resolution enhancement techniques, we have used objective assessment criteria, such as: PSNR (Peak Signal-to-Noise Ratio), and SSIM (Structural Similarity Index Measure) [16]. Different test images from mentioned databases with different image features are used for comparison of the proposal against other competitor algorithms. In this paper, the following families of classic wavelet functions are used: *Symlet* (Sym), and *Coiflet* (Coif).

Referring to the test image *Aerial-A,* the super-resolution results are exposed in Fig. 2 for designed and competitor techniques, reconstructing a 512x512 pixels resolution enhanced image from a LR 128x128 pixels image. The novel resolution enhancement algorithm appears to perform better in terms of objective criteria (PSNR and SSIM), as well as in terms of subjective perception, especially using wavelet *Sym-2*. The visual subjective perception can be verified in the zoomed part of the

Aerial-A image, where fine details appear to be preserved better in the proposed SR framework.

In the *SAR-S* image (Fig. 3), it is easy to see better performance in accordance with the objective criteria and via subjective visual perception in SR when our proposal is employed with the wavelet *Sym-2*. Novel algorithm presents better sharpness and less smoothing at the edges, blurred details, and ringing artifacts around edges.

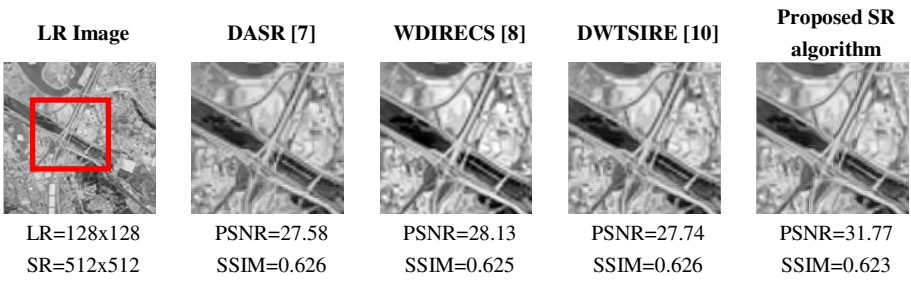

Fig. 2. SR results for the *Aerial-A* image contaminated by Gaussian noise (PSNR=17 dB)

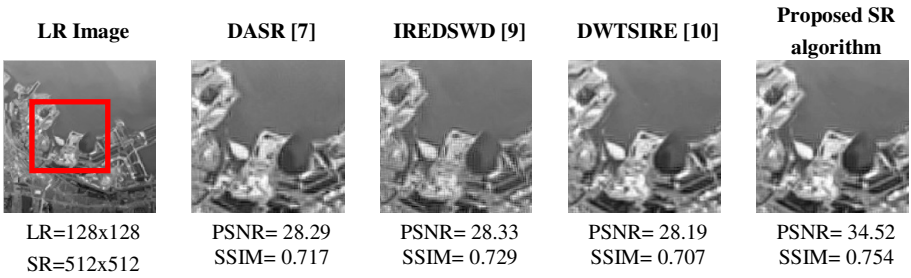

Fig. 3. SR results for the *SAR-S* image contaminated by Gaussian noise (PSNR=17 dB)

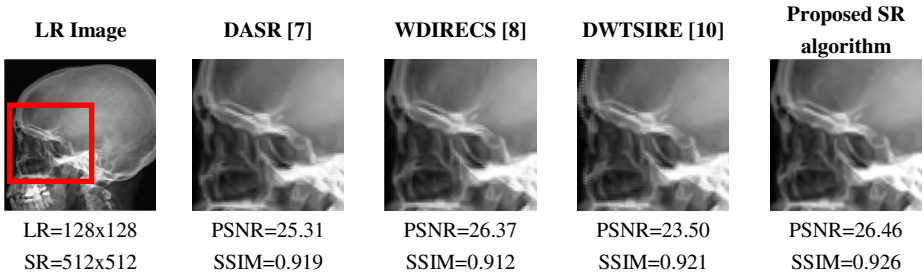

Fig. 4. SR results for the *Medical-M* image contaminated by Gaussian noise (PSNR=17 dB)

In the SR reconstructed *Medical-M* image, one can observe from analyzing Fig. 4 that the novel algorithm performs better in PSNR and SSIM criteria, especially using wavelet *Sym-2*, and presents a better perception especially in the well-defined borders (see the zoomed part of the image). The complete comparison evaluation of average objective measures (PSNR and SSIM values) throughout all images from the

databases ([11] and [12]) for the designed framework and competitor techniques has confirmed the best quality of our proposal: PSNR = 31.12 dB and SSIM = 0.672 against PSNR =28.62 dB and SSIM = 0.614 for the better SR algorithm DASR [7]. Given that the textures and chromaticity properties of the test images are different, the performance results confirm the robustness of the current proposal.

Table 1. Objective criteria results of the resolution enhancement from 128x128 to 512x512

Resolution-Resolution Algorithms		Aerial-A		SAR-S		Medical-M	
		PSNR	SSIM	PSNR	SSIM	PSNR	SSIM
IREDSWD [9]	Sym-2	27.02	0.577	28.33	0.729	22.94	0.904
	Coif-1	26.99	0.535	27.92	0.703	20.33	0.837
DWTSIRE [10]	Sym-2	27.74	0.626	28.19	0.707	23.50	0.921
	Coif-1	27.64	0.594	28.18	0.687	21.46	0.873
DASR [7]	Sym-2	27.58	0.626	28.29	0.717	25.31	0.919
	Coif-1	27.49	0.601	27.99	0.706	23.37	0.879
WDIRECS [8]	Sym-2	28.13	0.625	27.91	0.680	26.37	0.912
	Coif-1	27.78	0.587	27.93	0.661	24.06	0.909
PROPOSED SR TECHNIQUE	Sym-2	31.77	0.623	34.52	0.754	26.46	0.926
	Coif-1	31.78	0.613	34.53	0.745	24.13	0.911

5 Real Time Implementation

The designed framework that appears to demonstrate the best quality performance has been implemented in different hardware to demonstrate the possibility processing an image in real-time mode using a DSP (TMS320DM648), CPU i7-3770 (3.4 GHz), and GPU (NVIDIA® Quadro® K2000: CUDA Parallel-Process. Cores: 384, Frame Buffer Memory: 2 GB-GDDR5) platform. In first hardware, using MATLAB's Simulink™ module, a SR project was created, in which the DSP model EVM DM648™ and its respective task BIOS were selected.

Table 2. The processing time values for GPU, DSP and PC, i7-3770 processor

IMAGES	HARDWARE	PROCESSING TIME	POWER CONSUMPTION
Aerial-A	NVIDIA® Quadro® K2000	0.391 sec	51 W
	CPU i7-3770 (3.4 GHz)	1.083 sec	166 W
	DSP DM648 (900 MHz)	2.479 sec	5.02
SAR-S	NVIDIA® Quadro® K2000	0.391 sec	51 W
	CPU i7-3770 (3.4 GHz)	1.083 sec	166 W
	DSP DM648 (900 MHz)	2.479 sec	5.02 W
Medical-M	NVIDIA® Quadro® K2000	0.323 sec	51 W
	CPU i7-3770 (3.4 GHz)	1.021 sec	166 W
	DSP DM648 (900 MHz)	2.411 sec	5.02

Processing time values were computed for GPU, MATLAB™ and DSP hardware implementations. Table 2 exposes the processing time values for analyzed framework performing resolution enhancement for all three mentioned hardware. Here, the tested images were: *Aerial-A, SAR-S* and *Medical-M* (initial format: 128×128 pixels, output format 512×512 pixels).

The presented processing time values in table 2 are consistent with the devices speeds; this is because the CPU is faster than the DSP processor, but on other hand, the DSP module has in more than 30 times less power consumption. The third implementation on the GPU (NVIDIA Quadro K2000) platform is the fastest one because it can work performing framework operations in parallel.

6 Conclusions

In this study, a novel resolution-enhancement technique based on the interpolation of the HF sub-band images in the wavelet domain and the input image via sparse interpolation has been presented. In contrast with state-of-the-art algorithms, the designed framework applies the edge and fine features information obtained from the HF sub-band images in wavelet transform space, involving them in the SR restoration process. The designed technique has been tested on well-known benchmark images, presenting its superior performance in terms of objective criteria, as well as in the subjective perception via the human visual system. The quality analysis of the designed framework has been performed on DSP and on GPU platforms demonstrating the possible real-time application of the SR technique.

Acknowledgments. Authors would like to thank Instituto Politécnico Nacional (IPN) and Consejo Nacional de Ciencia y Tecnología (CONACYT) for the given support.

References

1. Bovik, A. (ed.): Handbook of Image and Video Process. Academic, MA (2000)
2. Shkvarko, Y.V., Tuxpan, J., Santos, S.R.: High-resolution imaging with uncertain radar measurement data: A doubly regularized compressive sensing experiment design approach. Proc. IEEE, 6970–6976 (2012) ISBN: 978-1-467311-51/12
3. Shkvarko, Y.V., Tuxpan, J., Santos, S.R.: Structured Descriptive Experiment Design Regularization based Enhancement of Fractional SAR Imagery. Sign. Proc. 93(12), 3553–3566 (2013)
4. Temizel, A., Vlachos, T.: Image resolution up-scaling in the wavelet domain using directional cycle spinning. J. Electron. Imaging 14(4), 040501 (2005)
5. Chavez-Roman, H., Ponomaryov, V.: Super Resolution Image Generation Using Wavelet Domain Interpolation with Edge Extraction Via a Sparse Representation. IEEE Geoscience and Remote Sensing Letters 11(10), 1777–1781 (2014), doi:10.1109/LGRS.2014.2308905
6. Hou, H.S., Andrews, H.C.: Cubic spline for image interpolation and digital filtering. IEEE Transactions on Signal Processing 26, 508–517 (1978)
7. Anbarjafari, G., Demirel, H.: Image Super Resolution Based on Interpolation of Wavelet Domain High Frequency Sub-bands and the Spatial Domain Input Image. ETRI Journal 32(3), 390–394 (2010)

8. Temizel, A., Vlachos, T.: Wavelet domain image resolution enhancement using cycle-spinning. Elect. Lett. 41(3), 119–121 (2005)
9. Demirel, H., Anbarjafari, G.: Image Resolution Enhancement by Using Discrete and Stationary Wavelet Decomposition. IEEE Trans. Image Processing 20(5), 1458–1460 (2011)
10. Demirel, H., Anbarjafari, G.: Discrete Wavelet Transform-Based Satellite Image Resolution Enhancement. IEEE Trans. Geoscience and Remote Sensing 49(6), 1997–2004 (2011)
11. http://peipa.essex.ac.uk/benchmark/databases/index.html
12. http://sipi.usc.edu/database/
13. Protter, M., Elad, M., Takeda, H., Milanfar, P.: Generalizing the nonlocal-means to super-resolution reconstruction. IEEE Trans. Image Process. 18(1), 36–51 (2009)
14. Mallat, S., Yu, G.: Super-Resolution with Sparse Mixing Estimators. IEEE Trans. on Image Process. 19(11), 2889–2900 (2010), doi:10.1109/TIP.2010.2049927.
15. Feng, L., Suen, C.Y., Tang, Y.Y., Yang, L.H.: Edge Extraction of Images by Reconstruction Using Wavelet Decomposition Details at Different Resolution Levels. Int J. Patt. Recogn. Artif. Intell. 14(6), 779–793 (2000), doi:10.1142/S0218001400000519
16. Wang, Z., Bovik, A., Seikh, H., Simoncelli, E.: Image Quality Assessment: From Error Visibility to Structural Similarity. IEEE Trans. Image Process. 13(4), 600–612 (2004)